Lawrence Berkeley National Laboratory
LBL Publications

Title

Kinetics of Clustering Reactions

Permalink

https://escholarship.org/uc/item/9rb698cc

Authors

Pundarika, E S

Morris, J W

Publication Date

1978-11-01

KINETICS OF CLUSTERING REACTIONS

E. S. Pundarika and J. W. Morris, Jr.

November 1978

DISCLAIMER

KINETICS OF CLUSTERING REACTIONS

E. S. Pundarika and J. W. Morris, Jr.

Department of Materials Science and Mineral Engineering and,

Materials and Molecular Research Division, Lawrence Berkeley Laboratory
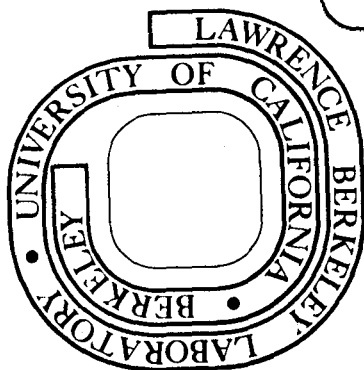
University of California, Berkeley, California 94720

ABSTRACT

The dynamics of precipitation and coarsening reactions in a binary Ising lattice are studied using a simulation technique. The initial random configuration of atoms represents equilibration at a very high temperature. Following a quench to a temperature below the miscibility gap, the decomposition proceeds by atomic interchanges of matrix and impurity atoms, as in the currently popular Kawasaki spin exchange model. Both the excess energy $<\epsilon-\epsilon_\infty>$ and the average cluster size $<n>$ are found to obey simple power law relations with time, $<\epsilon-\epsilon_\infty>=t^{-b}$, and $<n>=t^a$. For the square lattice, Binder's cluster diffusion and coagulation mechanism is seen to dominate the coarsening reactions at early times, in agreement with the studies of Lebowitz, et. al. The early time exponent (a) correspondingly has a value close to 0.2. However, at later times, the mechanism changes over to a Lifshitz and Slozov atom by atom transfer mechanism, as the cluster sizes become larger. The nature of this changeover is seen to depend principally on the temperature; the two regions overlap at higher temperatures, and are separated by a long incubation period at lower temperatures.

INTRODUCTION

A wide variety of metallurgical phenomena such as precipitation hardening and aging processes in alloys, and void formation and swelling in irradiated materials are controlled by the nature and kinetics of precipitation and coarsening processes. Theoretical analysis of diffusion controlled coarsening [1-3] and surface controlled coarsening[3] have given useful insight into these processes. These theories are based on free energy vs composition plots, are basically continuum in nature, and consider global equilibrium conditions. Spherical particles are assumed and composition effects are neglected. (Discussions of the effects of particle shapes can be found in reference 4 and of composition in reference 5). However, a thorough understanding of these processes can only be achieved through theoretical studies at the atomic level.

The advancement of high speed computer technology has made possible another method of approach: direct computer simulation of the atomic diffusion process. This approach, on the one hand, makes it easy to follow through the reactions step by step, without having to make any further assumptions, and facilitates greater understanding of the mechanisms involved. On the other hand, it represents the most clearcut 'experiments' that can be used to test the above mentioned theories[6] — physical experiments are replete with other parameters, and a complete assessment of the theories becomes infeasible. Previous studies of this type[8] have yielded a number of interesting results, and are continued in the work reported here.

Model

In this study we have used the spin exchange model originally used for studies of order-disorder transformations (see for example reference 7), in the simplest realistic case of a binary Ising lattice. Atoms of two types (A and B) are distributed over the available lattice sites and are assumed to interact only with atoms on nearest neighbor sites. A random distribution of A and B atoms represents, in this model, equilibrium at a very high temperature where the configurational entropy is dominant. (For an infinite lattice and for an infinite lattice only, this temperature is infinite). When the lattice is quenched from this high temperature to some low

temperature the atoms will assume a configuration of lower energy as dictated by the thermodynamics. This reaction will either be a clustering or an ordering reaction depending on whether the energy of the A-B interaction is such that the atoms have an energetic preference for neighbors of like kind or for neighbors of unlike kind. The kinetics of such reactions can be studied by a Monte Carlo type simulation by assigning jump probabilities [based on the temperature T and the change in energy ΔE of the system (proportional to the number of AB bonds) caused by the jump] to different atom exchanges and letting the reaction go as per the probabilities. Many different expressions have been used for the exchange probability P. In their original paper Metropolis et al[10] used values $P=1$ for $\Delta E < 0$ and $P=\exp(-\Delta E/kT)$ for $\Delta E > 0$. We have used the Boltzmann probabilities $P=\exp(-\Delta E/kT)/[1+\exp(-\Delta E/kT)]$. A recent study[11] has shown that the latter yields greater stability and faster convergence. An additional activation energy can be added to ΔE to account for the diffusion energy.

For our system, the Monte Carlo method consists of starting out with an initial random A-B distribution and the following steps:

(1) Choose an atom at random (from among all the atoms);

(2) Choose a neighbouring atom at random;

(3) Determine the jump probability P;

(4) Generate a random number R, $0 \leqslant R \leqslant 1$;

(5) Exchange if $R \leqslant P$;

(6) Repeat steps 1-5.

One trial per each lattice site measures one unit of time. Since the exchange probability of $\Delta E=0$ exchanges is 0.5, the average time between such exchanges would be two time units. Considering the diffusion coefficient D (at the reaction temperature) in the limit of zero concentration of B atoms (where all the exchanges would be of $\Delta E=0$) we see that 1 time unit $= a^2 \times (8D)$ where a is the lattice parameter.

This approach was used for studying ordering reactions as early as 1959, and has recently

gained importance in the study of clustering reactions. Whereas in the former case it was mainly used to study the equilibrium properties, in the latter case it is used to study the kinetics of clustering. Previous studies on this subject have been summarized in detail by Binder et al[8]. A recent study has employed this approach to study the kinetics of ordering reactions[9].

In the present work we have employed a slight variation of the Monte Carlo method, suitably modifying it to avoid unnecessary exchanges by considering only those exchanges that lead to a change in the microstructure. For each crystal structure there are only a few possible configurations of of AB bonds, and hence only a few possible values of P. The possible jump configurations can thus be classified into types of identical exchange probability and selected for exchange directly, with probability weighted by the population of each type. This method of simulation is much faster than the regular method, especially at low temperatures [see also section 2]. The seven different types of AB bond configurations for a square lattice are exemplified in Table I. The computing time necessary for a given number of AB exchanges depends only on the crystal structure (or, the number of neighbors). In the regular Monte Carlo method the computing time is a strong function of temperature, increasing exponentially as temperature is decreased. The slight temperature dependence in our case is actually in the opposite direction, the speed increasing somewhat at lower temperatures. Further, extension to the case including the second nearest neighbors also, involves only about a 40-80% increment in the computing time.

For the square lattice with nearest neighbor interactions only, the critical temperature for phase separation, T_c has been calculated exactly and is given by $T_c=2.414J$, where J is the interaction energy. Further the phase diagram is also available analytically, and is given by

$$C(phase) = \frac{1}{2} \left\{ \left[1 - \frac{16x^4}{(1-x^2)^4} \right]^{\frac{1}{8}} + 1 \right\}$$

where $x = \exp(-2J/kT)$.

TABLE I: BOND CLASSIFICATION

Type of bond (i)	Example of Configuration	Change in energy ΔE on exchanges/J	Probability of occurance at T=∞ and concentration C (N_i)	$N_i/\Sigma N_i$ for C=0.2 x100
1	A B A-B-A-B A B	-12	$4c^4(1-c)^4$	0.41
2	A B A-B-A-A A B	-8	$12[c^5(1-c)^3 + c^3(1-c)^5]$	5.2
3	A B B-B-A-A A B	-4	$12[c^6(1-c)^2+c^2(1-c)^6] + 36c^4(1-c)^4$	23.4
4	B A A-B-A-A A B	0	$4[c^7(1-c)+c(1-c)^7] + 36[c^5(1-c)^3+c^3(1-c)^5]$	41.9
5	B A A-B-A-B B A	+4	$12[c^6(1-c)^2+c^2(1-c)^6] + 36c^4(1-c)^4$	23.4
6	B A A-B-A-A B A	+8	$12[c^5(1-c)^3+c^3(1-c)^5]$	5.2
7	B A B-B-A-A B A	+12	$4c^4(1-c)^4$	0.41

Theory

The theoretical treatments of coarsening generally consider steady state, or very late stages of coarsening, where the coarsening rate is surface reaction controlled or diffusion controlled. The latter has been analysed in detail by Lifshitz and Slozov and is conveniently called Lifshitz-Slozov or LS mechanism. Coarsening here occurs by mass transport by single atom diffusion between clusters, driven by the eventual decrease in total surface energy.

Recently Binder[14] has analysed the coarsening of clusters by Binder's mechanism: diffusion and coagulation of clusters. His treatment is of a general nature without any explicit assumptions regarding the sizes, shapes or distributions of the precipitates. However, since the cluster diffusivities vary as $n^{-1} - ^{-1.5}$, Binder's mechanism should become less important as the average cluster size $<n>$ increases. The geometric features of the clusters which gain importance in the initial stages is not considered in these theories. For example the LS analysis assumes that the interfacial energy is independent of cluster size. This assumption is questionable at small cluster sizes, and the simulation results indicate that the cluster surface energy levels off after some cluster size. The LS theory also assumes spherical particles (isotropic surface tensions), but this assumption is not critical, as long as the particles have their equilibrium shapes[15].

Both the Binder and the LS mechanisms predict simple power laws for the variations of excess energy $<\epsilon - \epsilon_\infty>$ and average cluster size $<n>$ as follows:

$$<n> = t^a$$
$$<\epsilon - \epsilon_\infty> = t^{-b}$$

where

LS—   a = 0.66; b = 0.33

Binder—   a = 0.4-0.5; b = 0.2-0.25

It is thus possible to follow the manifestations of these mechanisms by following the slopes of $<n>$ vs t or $<\epsilon - \epsilon_\infty>$ vs t curves. In addition, in our simulation approach, we have the further advantage of being able to actually trace through the atomic steps and be able to
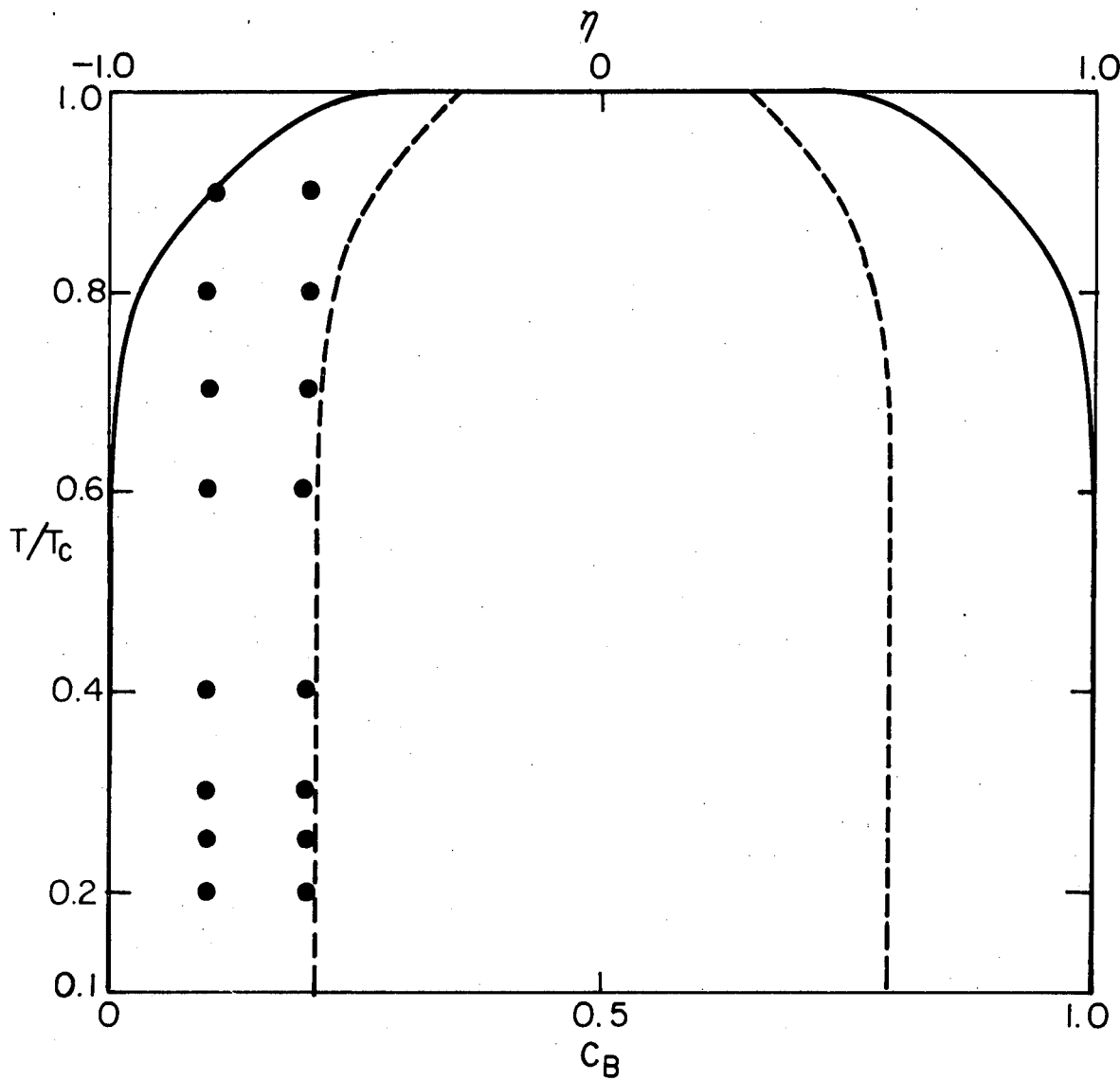
XBL 789-5834

Fig.1. Phase diagram of the binary Ising square lattice, indicating the points of simulation reported here. The dotted line shows the limit of metastability, assuming a free energy density of the form $f(C_{cr}) = A(C-C_{cr})^2+B(C-C_{cr})^4+f(C_{cr})$ where C_{cr} is the concentration at the phase boundary.

interpret the former results objectively. This advantage is especially significant at the small cluster sizes, since then the assumptions of neither theory (especially regarding the geometry of clusters) are satisfied.

Previous studies of this type have shown that Binder's mechanism dominates at the early stages of the process for the 2-d case[8]. It has also been pointed out that for the 3-d case, the LS mechanism should prevail at earlier times than in 2-d[6]. A slope change to a higher value corresponding to the LS mechanism at late stages in the $<\epsilon-\epsilon_\infty>$ vs t plots has also been reported. However, percolation effects hinder a meaningful study of the cluster sizes in 3-d[8].

RESULTS AND DISCUSSIONS

Figure 1 shows the phase diagram of a binary Ising lattice indicating the points of simulation reported here. Most of the simulations for square lattice were conducted on a 80×80 or 120×120 atom lattices, and for hexagonal lattice on 80×80 atom lattices. The coarsening reaction can be studied by following the variation of average cluster size $<n>$ with time. A plot of $<n>$ vs time is shown in Figure 2.

1. Basic Coarsening Reaction

Our results indicate that in the most general case the precipitation and coarsening reaction follows four stages.

(a) Initial Relaxation: Soon after the quench from the infinite temperature, the system tends to relax to a lower energy state. An example of this stage of the reaction is shown in Figure 3. Figure 3a shows the initial random configuration of a 20% B atom lattice, and Figure 3b shows the configuration after relaxation for 89 time units at $0.8 T_c$. [The location of A atoms are left vacant and the locations of B atoms are represented by dots]. Defining the precipitate to be a cluster of B atoms connected by nearest neighbor bonds, we see that in Figure 3b most of the B atoms have joined one or the other of the precipitates. Monomers and transient clusters such as dimers and trimers can be interpreted as dissolved in the matrix and show nearly equilibrium concentrations even at this early time. In fact it can be said that the phase separation reaction,
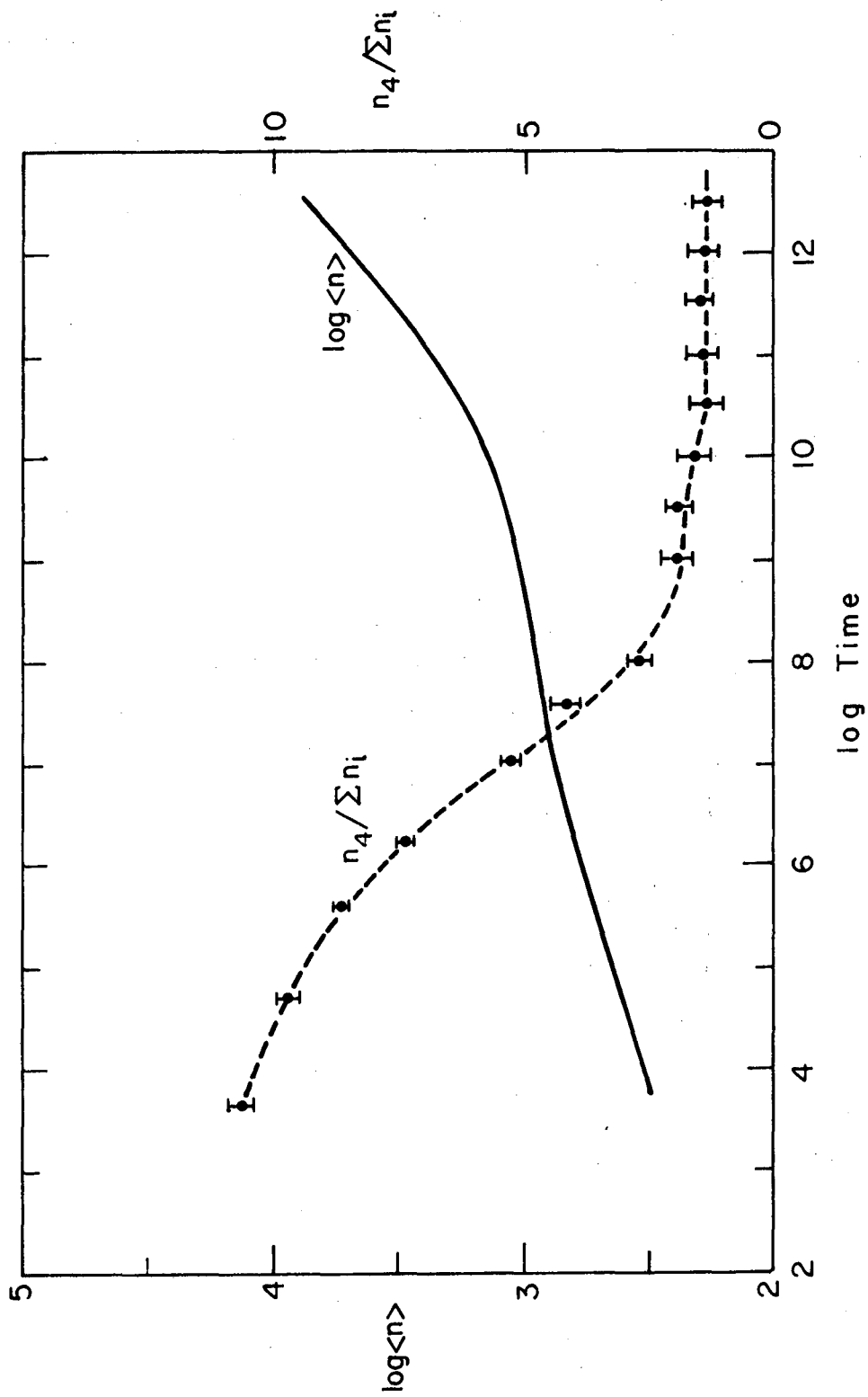
XBL 7811-6093

Fig. 2. Plot of average cluster size $\langle n \rangle$ vs time for a 120 x 120 square lattice of 20% B concen-

tration at a reduced temperature of $0.4T_c$. Also shown is the corresponding values of

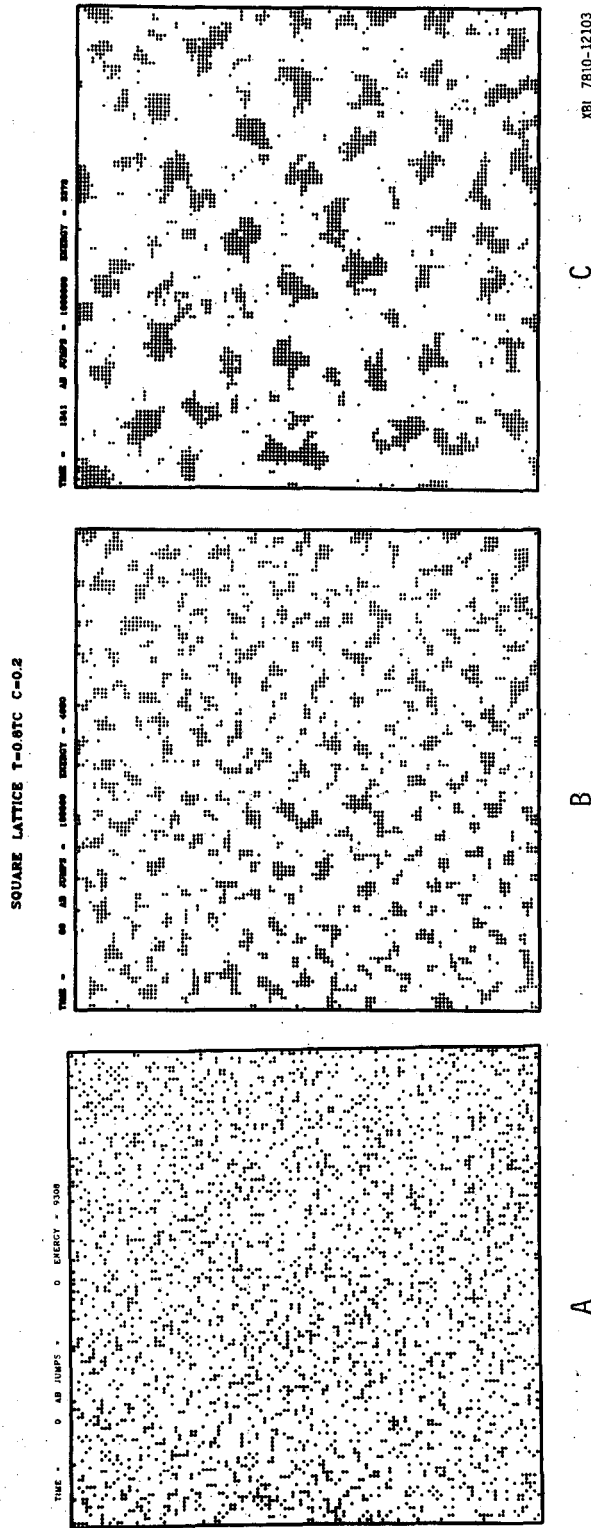relative bond population of bonds of type 4 (see Table I).

Fig.3. Time evolution of a 120×120 square lattice of 20% B concentration at $0.8T_c$. (a) Initial random configuration; (b) configuration after 89 time units and (c) Configuration after 1341 time units.

as dictated by the phase diagram is essentially complete at this stage. For comparison see Figure 3c which is a late time picture.

(b) Binder's Coarsening: This is essentially cluster coarsening by cluster diffusion and coagulation. When an atom chances to leave a cluster, it has a high probability of reattaching to the same cluster (in some other place); this leads to a shift in the centre of mass of the cluster, resulting in a random walk of the cluster through the lattice. This dynamic movement of clusters leads to their eventual collision and coagulation, resulting in an increase in the average size of the clusters. An example of this mechanism of cluster diffusion and coagulation is shown in Figure 4.

(c) Transition stage: This stage is characterized by a very small coarsening rate, especially significant at low temperatures. The reaction rate is basically controlled by the dissolution of atoms at precipitate surfaces. The seven different types of bonds (see Table I) reach constant relative populations $N_i/\sum N_i$ at the end of the transition stage. As an example, the variation of $N_4/\sum N_i$ with time is plotted on Figure 2, superimposed on the $<n>$ vs time plot. These constant relative populations depend on the temperature, and at infinite temperature they depend only on concentration, as listed in Table I.

(d) Lifshitz and Slozov coarsening: This is the usual Ostwald ripening occuring through atom by atom transfers from clusters to clusters, with diffusion through the matrix controlling the rate. This mechanism becomes predominant in the very late stages of the coarseing reaction and occurs at a rate faster than either (b) or (c).

A clearcut distinction into these four stages is not possible and there is always an overlap. The extent of overlap is temperature dependant and will be treated in a later section. The precipitates in the early stages are clearly non-spherical, and there exists a tendency towards spherodization as the reaction proceeds. Long thin clusters sometimes split into two or more in their efforts to spherodize. Sometimes a group of B atoms separate from a big cluster. These can then either redissolve in the matrix and redeposit on the surrounding clusters (LS mechanism) or can diffuse as a unit to join another cluster (Binder mechanism). This type of overlap
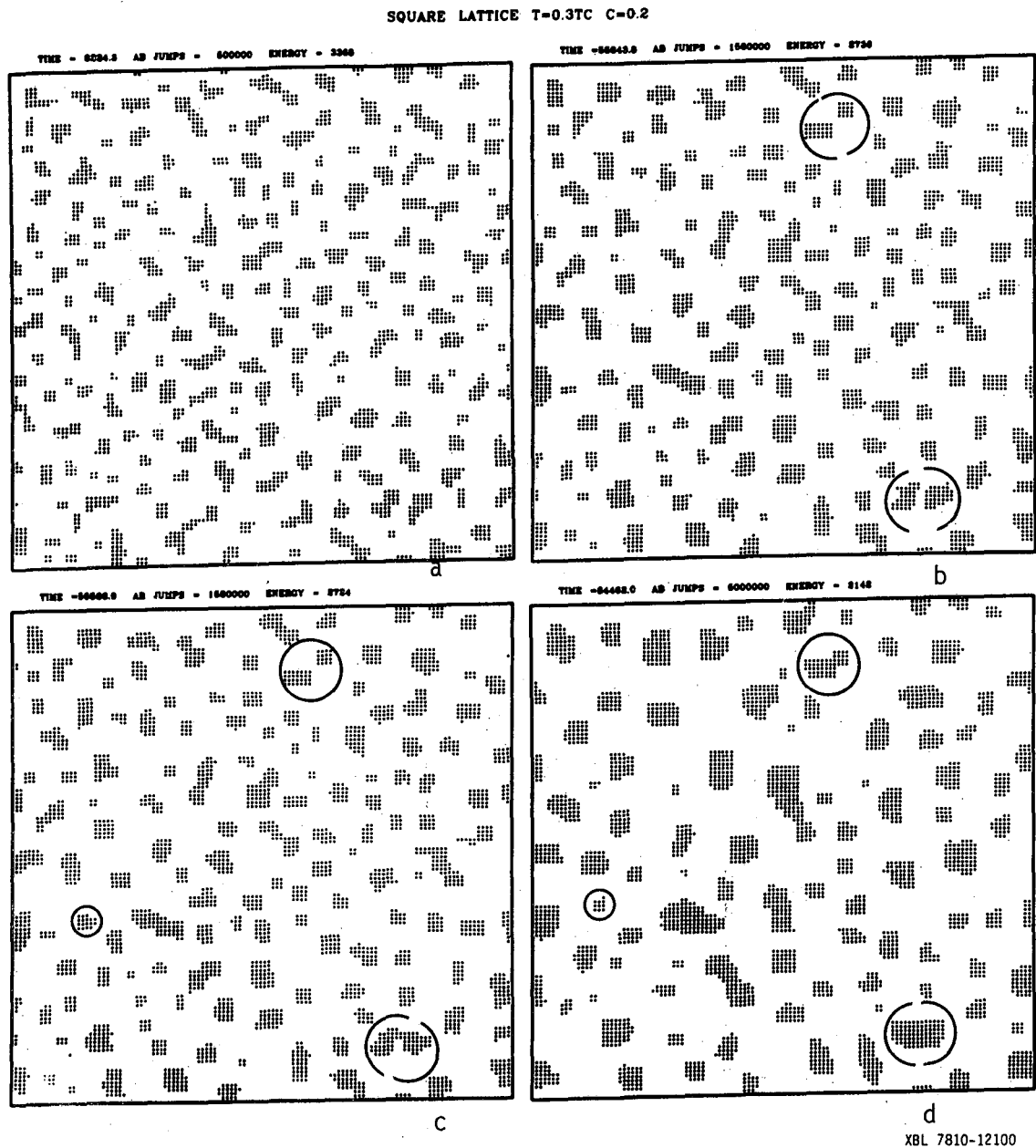
SQUARE LATTICE T=0.3TC C=0.2

Fig.4. Snapshots during the time evolution of a 120×120 square lattice of 20% B concentration at $0.3 T_c$ showing cluster diffusion and coagulation mechanism for example in regions marked with big circles. Notice also the atom by atom transfer mechanism, such as in the area marked with the small circle.

XBL 7810-12100

of mechanisms occurs almost at all times. Although the predominant mechanism is determined by the average cluster size, the path chosen by a particular cluster depends on its own size and its local environment.

2. Effect of Temperature

(a) Effect on overall kinetics: In this section we discuss the modifications in the general four stage coarsening scheme effected by temperature. Figure 5 shows the plots of average cluster size $<n>$ vs time at various temperatures for a 20% B atom alloy of 14400 atoms. Table II gives the exponents b of $<\epsilon-\epsilon_\infty> \propto t^{-b}$ at early, intermediate and late times. Whereas at medium temperatures all the four stages are present, at high temperatures stage 3 is absent, and at very low temperatures stage 4 is absent. At higher temperatures the change from Binder's to LS mechanism is rather gradual, both mechanisms overlapping over a wide range of times. At lower temperatures the two mechanisms are completely separated by a region of stage 3 with a slope lower than for either of the mechanisms; at short times 80% of the reaction is cluster diffusion and coagulation, and at long times 80% of the reaction is LS type. Further, the dimensionless time taken to reach steady-state or LS coarsening increases as we go down in temperature, with stage 3 extending further and further.

All these changes in kinetics with temperature stem from changes in (i) cluster geometry, (ii) relative jump probability, and (iii) matrix concentration of solute.

(i) Cluster geometry:

At high temperatures the clusters are rather diffuse, and seldom possess well defined boundaries until they reach larger sizes. The clusters at low temperatures are on the other hand much more compact. Figures 6a and 6b show the microstructures of a 20% B atom alloy in a square lattice at low $(0.4T_c)$ and high $(0.8T_c)$ temperatures. At roughly the same time after quench (since we use dimensionless diffusivities, the actual times at the low temperature would be much longer), the critical cluster size (which keeps on changing with time) is much smaller at the low temperature, and this leads to a high population of small sized clusters at $T = 0.4T_c$
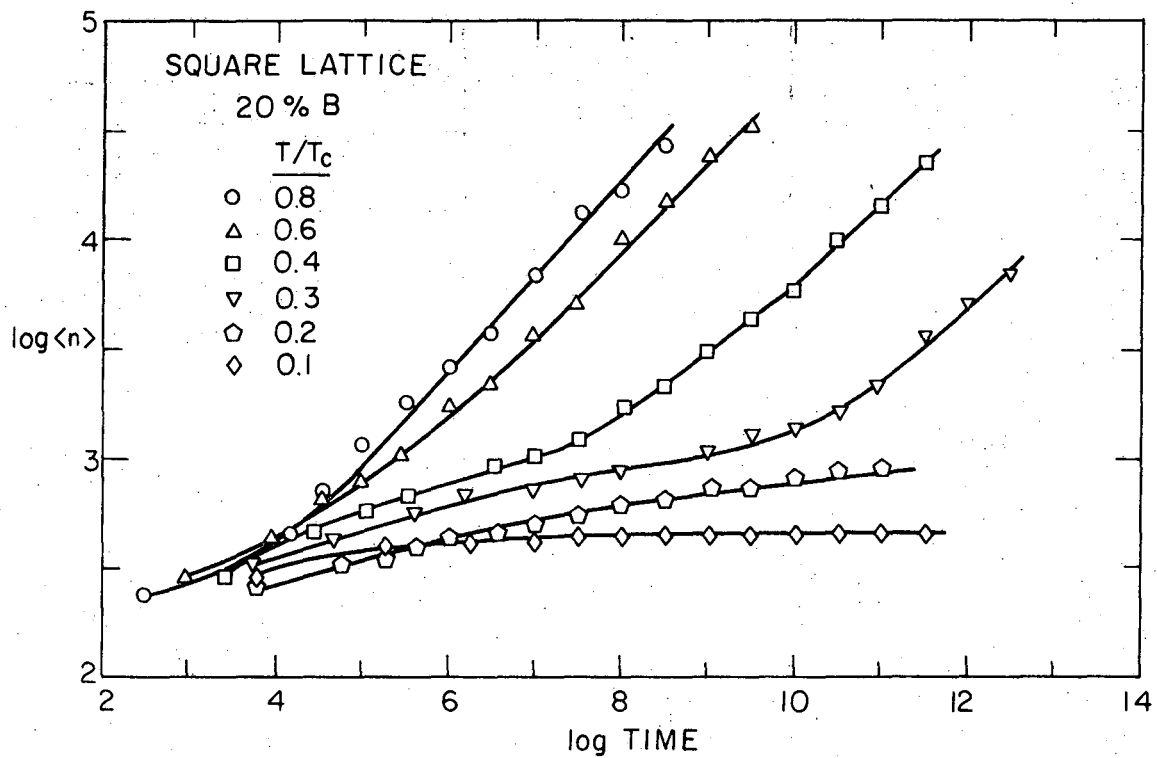
Fig.5. Plots of average cluster size $<n>$ vs time for a 20% B alloy at various temperatures. Note that the same dimensionless diffusivity is used for all the temperatures.

TABLE II. SLOPES b of $<\varepsilon-\varepsilon_{\infty}> = t^{-b}$

SQUARE LATTICE

T/T_c	EARLY TIME	INTERMEDIATE TIME	LATE TIME
		10%B	
0.8	0.14	0.18	0.26
0.6	0.16	0.22	0.29
0.4	0.17	0.13	0.33
		20%B	
0.8	0.16	0.24	0.14
0.6	0.16	0.21	0.28
0.4	0.15	0.13	0.28

LIFSHITZ AND SLOZOV

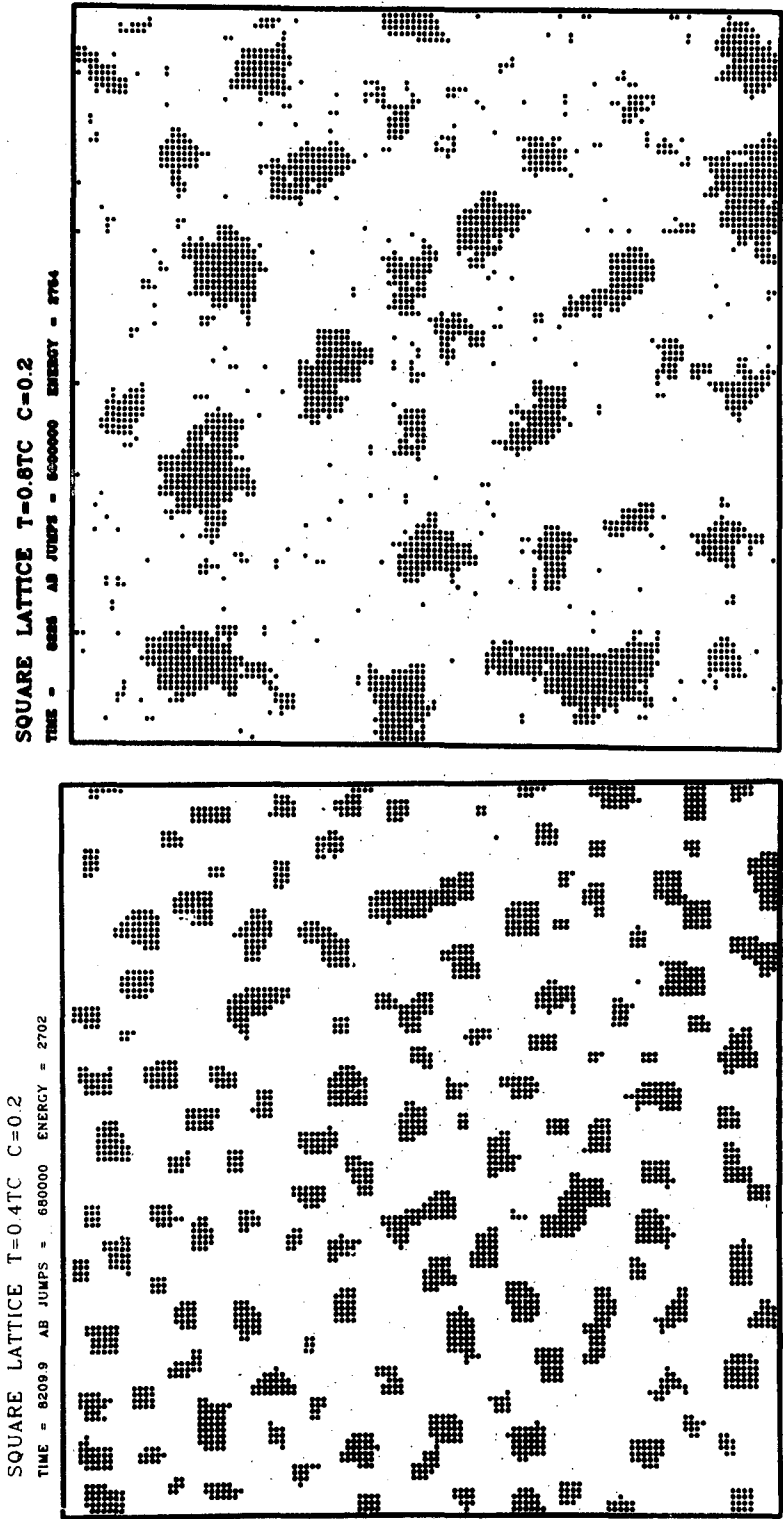| CLUSTER DIFFUSION AND COAGULATION	0.33
(A) SURFACE CONTROLLED CLUSTER DIFFUSION	0.2
(B) VOLUME CONTROLLED CLUSTER DIFFUSION	0.25

(Figure 6a). Further for $0.4T_c$ the equilibrium concentration in the matrix is much lower, as should be evident from the phase diagram.

More localized effects are observed at the lower temperatures. Each cluster tries to expose the face of lowest energy and this results in most of the clusters having (100) faces (which have only one exposed bond per surface atom). The average number of surface bonds per surface atom for an average cluster size of 60 atoms is about 1.6 for $0.8T_c$ and only 1.35 for $0.4T_c$. These numbers are for surfaces met with in our simulations. More precise numbers at any temperature can be obtained by studying the equilibrium profile of an initially straight infinite edge, in equilibrium with the equilibrium solute concentration at that temperature (obtained from the phase diagram).

The geometry of clusters at low temperatures has two important consequences:

(1) The geometrical relationship between the cluster volume and the cluster surface area (surface area $\propto n^{(d-1)/d}$ where d is the dimesionality) depends on the cluster compactness, and since the heart of the clusters are usually compact, on the cluster size. In other words, this geometrical relationship is satisfied at a much smaller cluster size at lower temperatures. For example, for $T = 0.9T_c$, n has to be $\geqslant 90$ for this relation to be valid, whereas at $0.4T_c$ it is valid for $n \geqslant 10$.

(2) The second more important consequence of geometry is its effect on cluster reactivity. Clusters with straight edges and sharp corners (i.e. square or rectangular clusters) are virtually inactive, until they gain an atom from some other cluster or, less commonly, lose an atom to the matrix, at which time they become "hyperactive", and they diffuse, dissolve, or change shape very dynamically until they again reach an inactive configuration. (This aspect was seen very well in the computer generated movies). At very low temperatures, all the clusters become inactive, whether rectangular or not. The resulting low reactivity at low temperatures results in the prolongation of stage 3 of the reaction. As the temperature is increased, i.e. as the clusters become more and more diffuse, and the matrix concentration of solute increases, stage 3 becomes shorter, and finally disappears.

SQUARE LATTICE T=0.4TC C=0.2

TIME = 8209.9 AB JUMPS = 680000 ENERGY = 2702

SQUARE LATTICE T=0.8TC C=0.2

TIME = 8209.9 AB JUMPS = 680000 ENERGY = 2704

A

B

XBL 7810-12102

Fig.6.　　Microstructure of a 20% B alloy at roughly the same time after quench to (a) $0.4T_c$

and (b) $0.8T_c$.

(ii) Relative jump probabilities:

The basic step in the coarsening reaction in our model is bond interchange. There are several types of bonds (seven types for the square lattice) with different values of interchange energy ΔE associated with their interchange (see Table I). The coarsening reaction is controlled by the probabilities of each of these types of bonds (this depends on the temperature and ΔE) and on their relative populations. Figure 7 shows the actual number of bonds that interchange with energy change ΔE per interchange. Whereas low energy jumps are not very sensitive to temperature, high energy jumps are "extremely" sensitive. It is seen from the figure that 94% of the jumps are of $\Delta E = 0$ at $0.3 T_c$ compared to 53% at $T = 0.8 T_c$. Comparatively, the population of the bonds of these types are 15% and 20% of the total bonds. The zero energy jumps correspond to either single atom movement on the cluster or single atom diffusion. For the case of $0.3 T_c$, it is 97% single atom movement of the cluster during stage 3 leading to some extent of cluster spherodization. Cluster diffusion, which usually involves high energy jumps, is lessened in this stage due to many clusters becoming inactive. The small diffusivity that still exists is responsible for the small extent of coarsening in this stage.

(iii) Matrix concentration of solute:

The solubility of the precipitate plays an important role in the coarsening reaction. For the Ising model the equilibrium concentration of solute atoms in the matrix keeps decreasing for T below T_c, and is nearly zero below about $0.4 T_c$ for the square lattice. Both the LS and Binder mechanisms work on the presumption of soluble precipitates. If the precipitates are nearly insoluble, atoms cannot leave the precipitate, and coarsening by the LS mechanism is extremely slow. Due to the compact geometry of the precipitates associated with low solubility, Binder's mechanism also becomes inoperative. Thus at very low temperatures we don't expect to see any significant amount of coarsening after the initial stages.

At somewhat higher temperatures, Binder's mechanism becomes operative at small cluster sizes, but clusters of larger size become inactive, i.e. Binder's mechanism decays. Due to the compact geometry of clusters and the low solubility, we have a situation where dissolution of
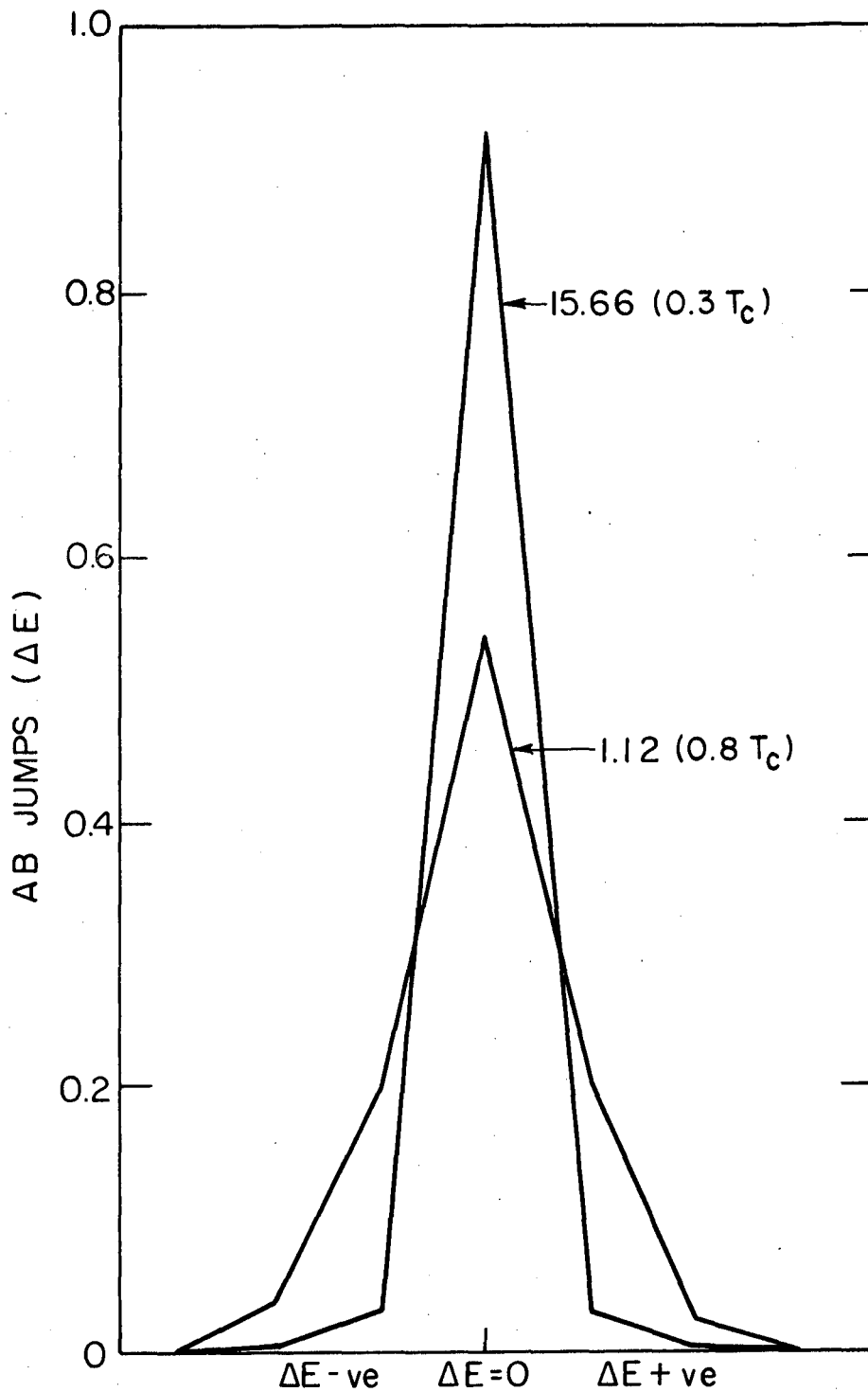
Fig.7.   Plots showing the fractional number of AB jumps of different types vs the energy

change involved in these jumps at $0.3T_c$ and $0.8T_c$. The numbers by the plots indi-

cate the ratio of AB jumps of $\Delta E = 0$ to AB jumps of $\Delta E \neq 0$.

atoms from the precipitate to the matrix is a difficult step. This leads to a "solubility controlled" coarsening. However, not all the clusters are completely inactive. Even clusters that are nearly square have or develop active centres such as kinks and double kinks which enable them to be more active in those regions. This leads at late times to a combination of "solubility controlled" (SC) and LS coarsening to occur.

(b) Effect of temperature on reaction rate: The role played by the geometry can be understood by separating it from (ii) and (iii). We can calculate the jump probabilities for each temperature and also the relative population of bonds, from which the expected reaction rate can be calculated. It is expected that the reaction rate will be different than the calculated rate: (1) at early times, because the initial bond populations are those typical of $T = \infty$ and it takes time to reach those typical of the experimental temperature; (2) at low temperatures, because geometrical restraints prevent or delay the reaching of steady state relative bond populations.

The reaction rate can be measured in terms of t^*, the time required for an AB exchange, which depends on the population of AB bonds and on the relative probability of an AB type jump vs an AA or BB type jump. The number of AB exchanges per unit time given by $1/t^*$ would be a good measure of the system reactivity R^*, since only such exchanges change the energy or microstructure of the system.

Based on the assumption that the bonds have reached constant asymptotic relative populations (typical of each temperature) in accordance with the energies associated with them, we can calculate the expected time per AB bond jump as

$$t^* = \left[\frac{N_{AB}}{N_{total}} \sum_i P_i N_i \right]^{-1} \tag{1}$$

where P_i are the jump probabilities of the types $i = 1,7$ and N_{AB} is the total number of AB bonds, N_{total} is the total number of bonds in the system and N_i is the partition factor which gives the fraction of the N_{AB} bonds in the various types. This formula predicts that at infinite temperature, $t^* = 1/f$ where f is the fraction of bonds of the AB type, $f = c(1-c)$, c being the impurity concentration. At any lower temperature, t^* is greater than this value. [If we had a

highly supersaturated solution, we can have $t^* \ll 1/f$ as happens at the beginning of the reaction. As time increases, t^* reaches values typical of each temperature]. At infinite temperature N_i is independent of the energy associated with each bond type, and depends oly on the multiplicity of the bond type (which in turn depends on the impurity concentration ad the lattice geometry). The calculations of N_i at infinite temperature and their values for a concentration of 0.2 are given in Table I. At any other temperature, the values of N_i are modified by a factor $\propto \exp{(\Delta E/kT)}$.

Figure 8 shows the plots of t^* vs T after 1×10^6 and 5×10^6 exchanges. The prediction given by equation (1) is also given. The expected deviations of the simulation results from the calculated values are observed in the figure. The deviations at lower temperatures can be explained by reference to Figure 6. Although N_{AB}/N_{total} keeps decreasing with temperature and the partition among the seven types of these N_{AB} bonds does tend to favor the lower energy types as we lower the temperature, at very low temperatures the system finds itself in a high energy position $(N_{AB}/N_{total} \gg \epsilon_\infty)$ which favors $\Delta E = 0$ bonds profusely. This means that the jump keeps occuring at higher frequencies, but N_{AB} does not decrease. Thus the system is frozen in a local state of neutral equilibrium of high energy and high reactivity, escape from which is difficult because of geometric restraints. When it does escape and move towards the equilibrium state, the t^* should follow the calculated curve.

When the system is quenched from infinite temperature to the reaction temperature it tries to (1) equilibrate the composition; (2) equilibrate the relative bond populations (surface profile); and (3) "minimize" energy. Equilibrium of composition is achieved at very short times at all temperatures. Equilibrium of relative bond populations is achieved at short times at higher temperatures but takes longer at lower temperatures. There is thus a competition between (2) and (3) at lower temperatures.

The reactivity R^* of the system $(=1/t^*)$ keeps decreasing with time. When the system enters the equilibrium state (which is dynamic) the reactivity reaches a constant value. By starting out with the equilibrium state at $T = 0$ (lowest energy state) and equilibrating at the
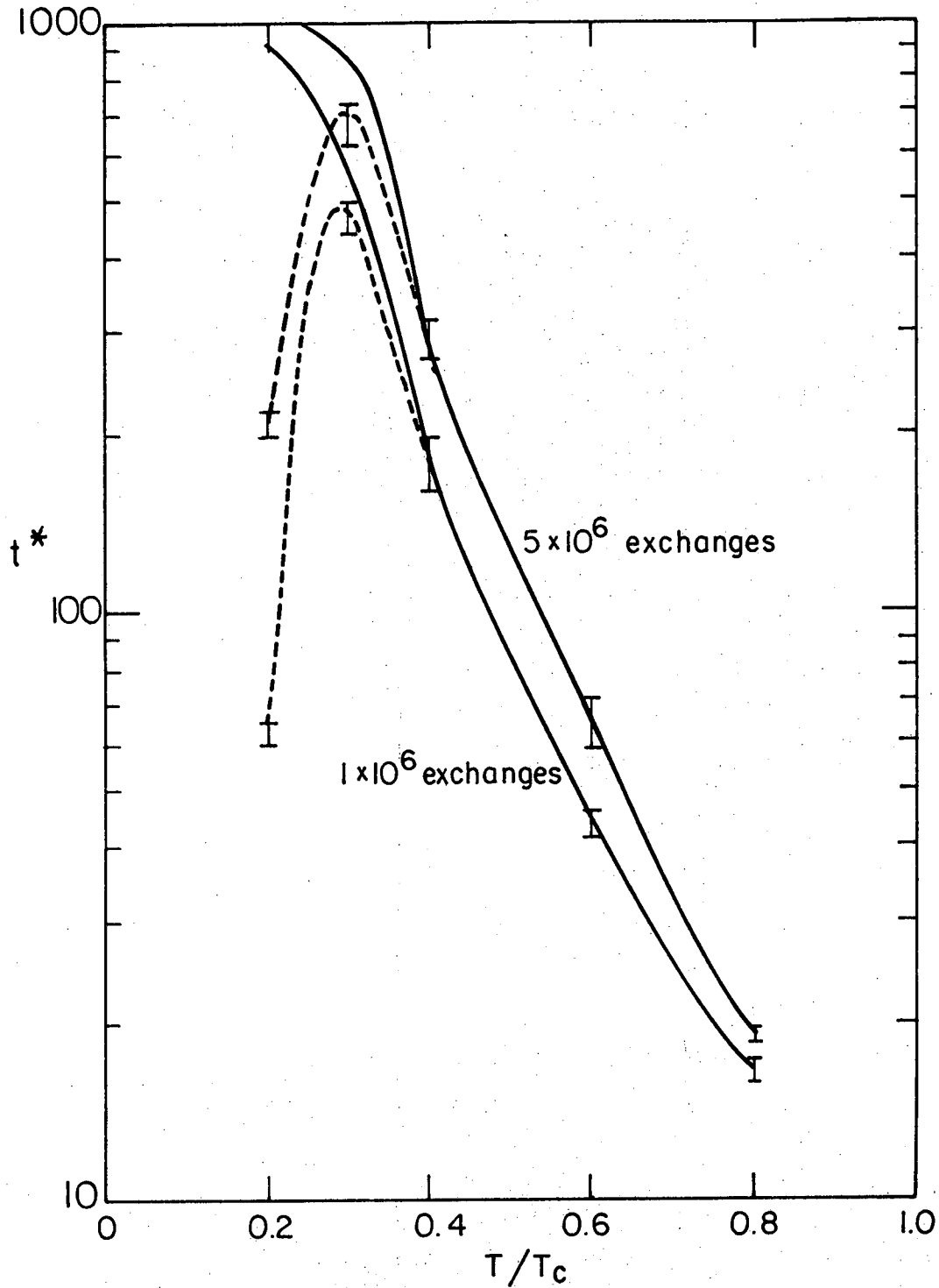
XBL 785-5053

Fig.8. The average time between successive AB jumps (t^*) vs temperature after 1×10^6 and

5×10^6 AB jumps. The data bars are simulation data, the continuous curves are

obtained from asymptotic bond populations, and the dotted curves indicate the devi-

ation.

reaction temperature, this final reactivity can be found. The reactivity at any time during coarsening at that temperature starting from the random initial configuration is them given approximately by $\frac{\epsilon}{\epsilon_\infty} \times R_\infty$. On Figure 9 the energy values (starting from the energy for random distribution) and the corresponding t^* values obtained from simulation are shown as data bars. The continuous curves are the t^* values calculated from $t^* = 1/R^* = \epsilon_\infty/(\epsilon \times R_\infty)$. That is, the continuous curves indicate the t^* values when the partition of bonds into types reaches a steady value, corresponding to the distribution in the equilibrium state. The point where the data bars reach the continuous curve signifies the time when the bond populations have reached a steady state, since the same distribution of bonds into types can be expected to be maintained through to the equilibrium state. When steady state bond populations are reached, the system is now only trying to reach "minimum energy" state, and this signifies the end of stage 3.

3. Effect of Composition

The general coarsening behaviour remains largely unchanged after changes in composition. However, composition has these four effects: (a) Higher composition means a bigger difference between the infinite temperature state and the experimental temperature state, and hence increases the initial relaxation period. (b) The cluster diffusion mechanism seems to be more predominant at higher compositions. (c) Table III shows the slopes of $<n> = t^a$ for 10% B and 20% B case at roughly the same time range. In the case of 10% B, a higher fraction of B atoms are in the matrix, aiding the freer flow of atoms between the particles, as also their diffusion. Thus the slopes are somewhat higher for the 10% case than for the 20% case. It is tempting to conclude that the reason for this could be because with 10% B the LS assumption of widely dispersed precipitates is better satisfied. However, Ardell's analysis[5] argues that the time exponent does not depend on the volume fraction of the precipitate. (d) Steady state bond populations are reached much faster at lower concentrations.
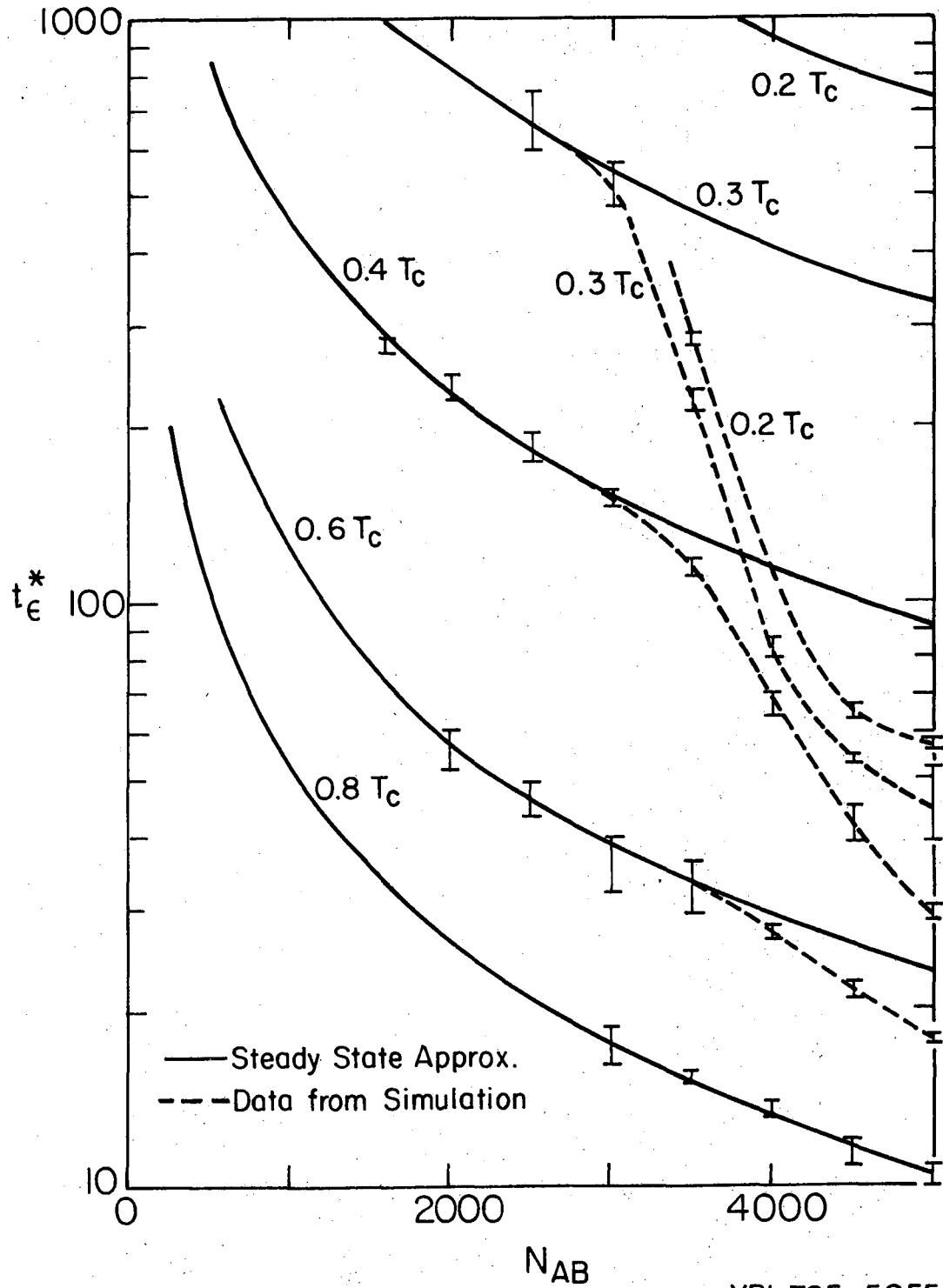
Fig. 9.   The average time between successive AB jumps (t^*) vs the number of AB bonds in

the lattice (N_{AB}). The data bars are simulation data, the continuous curves are

obtained from asymptotic bond populations, and the dotted curves indicate the devi-

ations.

TABLE III: SLOPES a OF $\langle n \rangle = t^a$

SQUARE LATTICE

T/T_c	10%B	20%B
0.9		0.39
0.8	0.67	0.40
0.7	0.56	0.40
0.6	0.44	0.40
0.4	0.46	0.36
0.3	0.33	0.32

LIFSHITZ & SLOZOV   0.66

CLUSTER COAGULATION

    (A)   SURFACE CONTROLLED CLUSTER DIFFUSION   0.4

    (B)   VOLUME CONTROLLED CLUSTER DIFFUSION   0.5
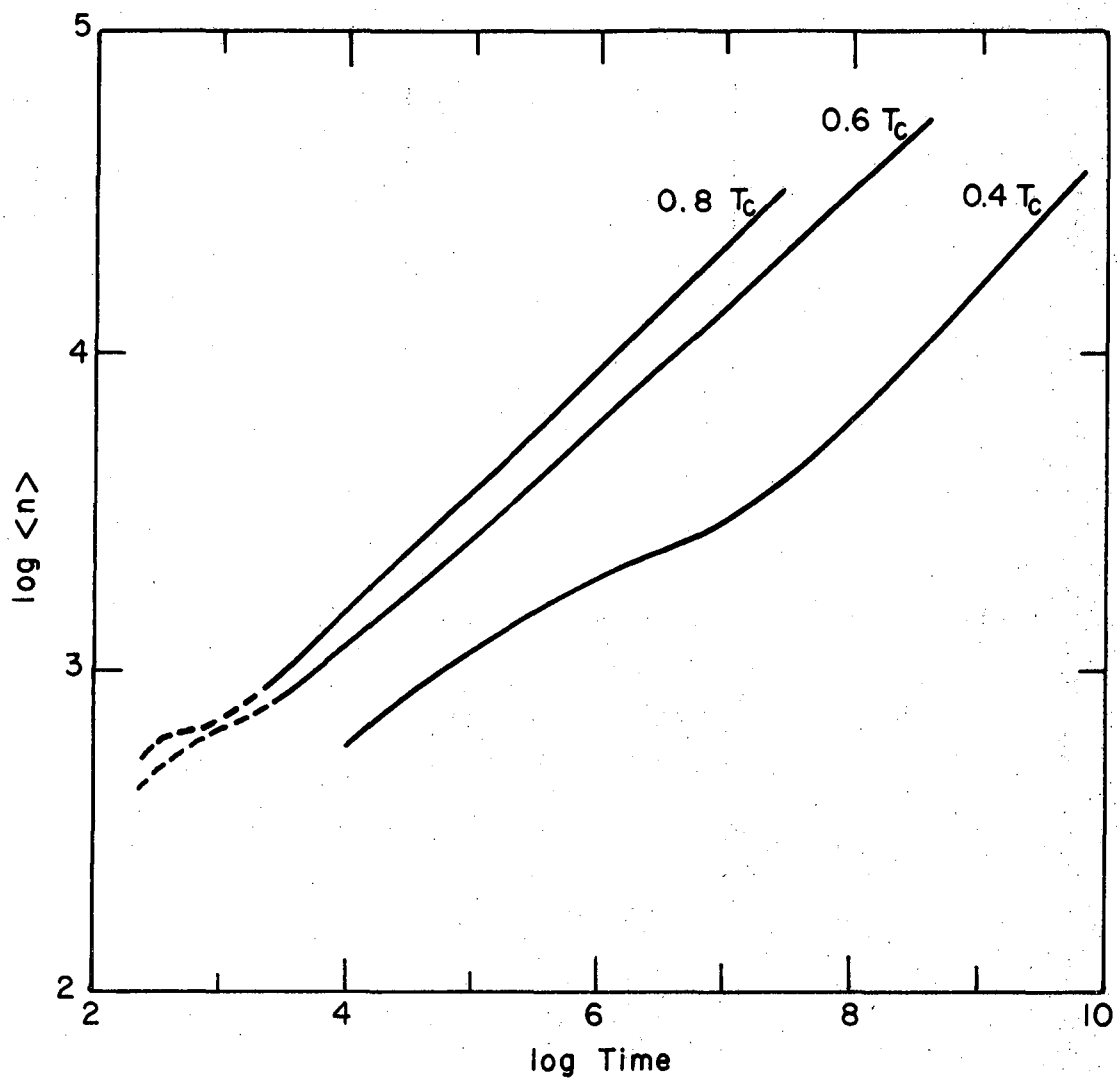
Fig. 10.   Plot of average cluster size $<n>$ vs time for a 80×80 hexagonal lattice of 20% B concentration.

4. Effect of Lattice Type

One other lattice type, the hexagonal lattice, was simulated. It differs from the square lattice in that in a hexagonal lattice the nearest neighbors of an atom are the nearest neighbors of one another unlike in the square lattice. This fact makes the number of bond types only 7 (instead of 13) in spite of the six nearest neighbor atoms. The phase diagram is also very close to that of the square lattice.

Regarding the kinetics of coarsening, the hexagonal lattice is not very different from the square lattice and shows the same four stage behaviour. Figure 10 shows an example of $<n>$ vs time curve for a hexagonal lattice. However, the geometry of the hexagonal lattice provides the possibility of cluster diffusion by zero energy jumps. For example a 2 atom cluster can diffuse without any high energy jumps here, which is impossible in a square lattice. This factor makes the Binder's mechanism more dominant at early times, the slopes corresponding much more closely to the predicted values. Also the smallest cluster unit during the frozen period at very low temperatures becomes 3 instead of 2 atoms. The slopes in stage 3 are in general higher than for the square lattice.

CONCLUSIONS

(1) Both excess energy $<\epsilon-\epsilon_\infty>$ and the average cluster size $<n>$ are found to obey simple power law relationships with time, $<\epsilon-\epsilon_\infty> = t^{-b}$, $<n> = t^a$, the exponents corresponding to LS mechanism at very late times.

(2) The general case of precipitation and coarsening in binary Ising square lattice follows four stages:

    (i)   initial relaxation

    (ii) Binder's mechanism (cluster coagulation)

    (iii) transition stage — cluster coagulation declines

(iv) LS and SC mechanisms set in, Ostwald ripening by diffusional processes.

(3) Temperature affects the general four stage mechanism in such a way that at very high or very low temperatures only three stages are seen. At high temperatures stage (iii) is almost absent and stages (ii) and (iv) overlap very much; as the temperature is lowered, stage (iii) becomes longer, and at very low temperatures stage (iv) is not reached in reasonable experimental time.

(4) Temperature also affects cluster geometry, the clusters being more compact and faceted at lower temperatures.

(5) Low temperature simulations, where solubility is low never reach significant coarsening rates, although the dimensionless diffusivity is the same as that at high temperatures. This suggests that clusters with very low solubility can resist coarsening.

(6) Temperature is also seen to affect the time taken to reach the constant asymptotic bond-type populations. This explains the unusual behaviour of t^* (average time between successive AB interchanges) with temperature.

(7) Although composition does not affect the general coarsening behaviour, a higher composition makes the particle growth kinetics a little sluggish. Also, the cluster diffusion and coagulation mechanism is seen to be more predominant at higher compositions.

(8) The coarsening kinetics on a hexagonal lattice are very similar to those on a square lattice.

ACKNOWLEDGEMENTS

REFERENCES

1. C. Wagner, *Electrochemie,* **65**, 243 (1961).

2. Lifshitz and Slozov, *J. Phys. Chem. Solids,* **19**, 35 (1961).

3. M. Kahlweit, *Colloid Interface Sci.,* **5**, 1 (1975).

4. C. A. Johnson, *Surface Science,* **3**, 429 (1964).

5. A. J. Ardell, *Acta Met.,* **20**, 61 (1972).

6. K. Binder, *Phy. Rev. B,* **V15**, 9, 4425 (1977).

7. L. D. Fosdick, **Methods in Computational Physics,** (B. Alder et al. eds. Academic Press, New York, 1963), V. 1.

8. K. Binder et. al. in **Nucleation Vol. III,** ed. Zettlemoyer (preprint).

9. Lebowitz, Phani and Tsai, AIME Winter Meeting, Feb 26-March 1, 1978, Denver, Colorado.

10. N. Metropolis et. al., *J.C.P,* **21**, 1087 (1953).

11. G. W. Guggenheim and P. H. B. Meijer, *J. Comp. Phys.,* **20**, 50 (1976).

12. K. Binder and D. Stauffer, *Adv. Phys.* (1976).

13. O. Penrose and J. L. Lebowitz, in **Nucleation Vol. III,** ed. Zettlemoyer (preprint).

14. K. Binder and D. Stauffer, *Phy. Rev. Lett.,* **33**, 1006 (1974).

15. G. W. Greenwood, **The Mechanism of Phase Transformations in Crystalline Solids,** Inst. of Metals Monograph #33, 103 (1969).